Impact of Some Discontinuities on the Convergence Of Numerical Methods in Electromagnetics.

Malcolm M. Bibby
Gullwings, Weston, MA 02493
e-mail: mbibby@gullwings.com

Abstract. The effect of discontinuities at edges and at feed-points of antennas on numerical convergence rates is investigated. In the case of edges, higher order representations of the edge-mode, expressed with the aid of Hermite splines, are shown to provide improved convergence in both global and local measures. When using a magnetic frill to excite an antenna, it is shown that when the current representation allows for the "charge jump" across the frill, then convergence is accelerated. The use of both sub-domain and entire-domain functions is explored.

Introduction.

The treatment of edge conditions in electromagnetic problems is generally thought to be well understood, particularly after the publication by Meixner [1] of the relationship between 'edge angle' and the power of the distance from the discontinuity. An extensive review by Van Bladel [2] brought together much of the evidence in support of the phenomenon's existence. Nevertheless, the model proposed by Meixner, while widely accepted, has not benefited from further development. More recently, Shen, et al., [3][4] reported on an analytical solution for the current and charge distributions at the ends of a tubular dipole. Their work showed that the Meixner method applied only at the very ends of such a dipole. While extending our knowledge in this area, their work is, nevertheless, restricted to current/charge distributions on a tubular dipole.

A different form of discontinuity arises at the feed-point of an antenna. This fact is less well recognized. The author knows of only one report that discusses it quantitatively. In this report, Popovic, Dragovic and Djordjevic [5, p38] pointed out that "as a consequence of the annular magnetic-current frill excitation, the current derivative has a discontinuity at the frill location". They then went on to quantify the charge jump that occurs in this situation. Unfortunately, it is not clear, from the balance of their writing, how they consistently incorporated this observation into their work in a general manner.

Recently, the author published reports [6][7] that examined the use of higher order basis functions in modeling a tubular dipole antenna/scatterer. The results presented in these reports did not support the expectation that higher-order basis functions would provide faster convergence properties. The models used in these investigations employed splines up to fifth order. They also incorporated the Meixner edge condition. Subsequent analysis has shown that the application of the simple form of the edge condition actually inhibited the convergence properties of the higher order models. The simple form of the Meixner edge condition has only one degree of freedom - it's amplitude. In order for the splines covering the rest of the antenna/scatterer to meet their potential, the number of degrees of freedom in the edge model were increased (in this study) to match those of the adjacent spline.

As part of the analysis referred to in the preceding paragraph an appreciation for the problem associated with the charge jump across the magnetic frill developed. The problem exhibits itself through a slow convergence and/or oscillation in the input admittance of the antenna as the model size is increased. The slow convergence problem was found to occur for both entire-domain and sub-domain basis functions.

The Basis Functions.

The sub-domain basis functions used on the main portion of the antenna/scatterer are all splines and are shown in Table I. They are the same as those used in [6][7]. They include the linear spline, which acts as a reference for the performance of the higher-order functions. As the results when using the 3-term-sin/cos

1054-4887 © 2003 ACES

Expansion Function	Mathematical Description
3-term sin/cos	$I(y) = A_i + B_i \sin(k(y - y_i)) + C_i(\cos(k(y - y_i) - 1)$ where $y_i \le y \le y_{i+1}$
Linear Spline	$I(y) = a_i + b_i(y - y_i) \quad y_i \le y \le y_{i+1}$
Quadratic Spline	$I(y) = a_i + b_i(y - y_i) + c_i(y - y_i)^2 \quad y_i \le y \le y_{i+1}$
Cubic Spline	$I(y) = a_i + b_i(y - y_i) + c_i(y - y_i)^2 + d_i(y - y_i)^3$ where $y_i \le y \le y_{i+1}$
Quartic Spline	$I(y) = a_i + b_i(y - y_i) + c_i(y - y_i)^2 + d_i(y - y_i)^3 + e_i(y - y_i)^4$ where $y_i \le y \le y_{i+1}$

Table I. Definitions of the splines considered in this study.

$$a_{N+1} = \sum_{i=}^{N} c_i \Delta_i^2 + 2\sum_{i=1}^{N-1} c_i \Delta_i \sum_{j=i+1}^{N} \Delta_j + b_1 \sum_{i=1}^{N} \Delta_i + a_1 \quad (1a)$$

$$b_{N+1} = 2\sum_{i=1}^{N} c_i \Delta_i + b_1 \quad (1b)$$

functions were almost identical to those found when using the quadratic spline, only the latter are reported. The reader should be aware however that the 3-term-sin/cos functions were studied. When using splines such as those found in Table I, one asserts as much continuity at the junction of contiguous cells as the functions allow. For example, a quadratic spline, which is of order 3 and degree $p = 2$, provides C^1 continuity. Hence, in the case of a quadratic spline both the amplitude and the first derivative can be matched. By this means the number of variables is reduced. In the case of the quadratic spline, for N cells, one needs to determine only the free variables $a_1, b_1, \sum_{i=1}^{N} c_i, b_{N+1}, a_{N+1}$. The amplitude and first derivative at one extremity are related to those at the other extremity through the relationships given in equations (1a) and (1b) above.

The sub-domain edge/end basis functions used in this study are based on the form given in [2, p120]:

$$E_z = d^v(a_0 + a_1 d + a_2 d^2 + a_3 d^3 + ...) \quad (2)$$

where E_z is the electric field normal to the edge/end, d is the distance from the edge/end, v is a number greater than –1.0 and the series $a_0, a_1, a_2, a_3, ...$ are constants to be determined. Expression (2) needs to be matched up, at its cell boundary, with each of the functions shown in Table I. Thus derivatives of this function are required. Straightforward differentiation of the function can be performed no more than once while still maintaining a function that can be integrated, and thus might be employed with the quadratic spline. However, it would fail for higher order splines. An alternative, and numerically superior, method is to apply the concepts found in the development of Hermite splines.

Hermite splines are different from most splines found in computational electromagnetic studies which are concerned only with amplitudes. The splines in Table I are examples of this latter situation. The constants at the open ends of these splines are the source of much writing on ways to handle them. – see, for example, [8]. The derivatives of these splines are functions of these constants. In the development of Hermite splines the issue of derivatives is tackled directly. Hermite splines are typically of odd degree, including $p = 1$, and are defined in terms of their amplitude and $(p - 1)/2$ derivatives at each end. The process for developing Hermite cubic splines is covered in [9] and the more general case, with applications to CEM, is described in [10]. In the case of equation (2) only one end is open and the development for a two term expression will be described next. Two terms will provide amplitude, $f(1)$, and derivative, $f'(1)$, information that can be used directly with the quadratic spline described earlier.

Equation (2) is restated as $P(u) = f(1)H_1(u) + f'(1)H_2(u)$, $u = \left(\frac{h - z'}{\Delta}\right)$, $(h - \Delta) \le z' \le h$, Δ is the width of the cell and h is identified with a cell boundary. $H_1(u)$ is a polynomial of order 2 selected so that $H_1(1) = 1$ and $H_1'(u) = 0$. Similarly, $H_2(u)$ is a similar polynomial selected so that $H_2(1) = 0$ and $H_2'(1) = 1$. When these conditions are applied, the solution is given by:

$$P(u) = u^{\nu}((1 + \nu) - \nu u)f(1) + u^{\nu}(1 - u)\Delta f'(1) \quad (3)$$

This provides us with what we are looking for – a function that separates the amplitude and the first derivative at the open end and one that can be integrated in a straightforward manner. This concept can be extended to functions of higher orders, and is done in this study for use with the cubic and quartic splines of Table I.

When investigating the discontinuity at a magnetic frill, a structure that possesses no other discontinuities is useful for investigative purposes. A circular loop is such a structure and is examined here. The 'natural' basis functions to use in this situation are Fourier series. Due to symmetry, only cosine terms are typically used. The expansion series is then:

$$I = \sum_{i=0}^{N} a_i \cos(i\phi) \quad 0 \le \phi \le 2\pi \quad (4a)$$

This expansion has been in use for decades and the results of its use are well documented [11]. When one examines the reported results, the lack of finality in the convergence of the admittance at the feed-point is notable. Zhou and Smith [12] attributed this poor convergence to the use of a delta-function source. Their results using a magnetic frill source demonstrated that indeed the frill source performed better than the delta-function source. However the admittance curves still did not fully converge until N in (4a) was extremely large. This is surprising given the 'natural' suitability of the functions in (4a). The work reported here shows that the model in (4a) is deficient for use when dealing with the magnetic frill as it does not account for the 'charge jump' across the frill. The derivatives of (4a) are all continuous, and what is needed is a set of functions that allows for this 'charge jump'. Instead of discarding (4a), one can modify it as in (4b) below.

$$I = a_0 + \sum_{i=1}^{N} (a_i \cos(i\phi) + b_i \sin((2i - 1)|\phi|/2)) \quad (4b)$$

The derivatives of this series are such that a 'charge jump' can be modeled properly. As discussed in [10], in the immediate vicinity of the frill it is the odd derivatives of the current that must be in anti-phase on opposite sides of the frill.

Solution Tools

The equations used in the analysis that follows are based on the Electric Field Integral Equation, EFIE, formulation. In particular, in the case of the linear dipole, the equation is Hallen's derivation [13], shown in (5) below. In (5) I is the desired current, G is the Green's function, $R = \sqrt{(z - z')^2 + (2a\sin(\frac{\phi'}{2}))^2}$, the radius is a, C is a constant to be determined and E_i is the incident excitation. The dipole, which is an open circular cylinder with an infinitesimally thin wall thickness, is located with its center at the origin of a cylindrical coordinate system with its length aligned with the z axis.

When investigating the loop, the derivation due to Mei [14], specialized for a loop is used – see (6) below. The center of the loop is located at the origin of a cylindrical coordinate system, with $s = R_b\phi$. The loop itself lies in the ρ,ϕ plane with its feed-point at $\phi = 0$. In this case, the expression for R in G is $R = a^2 + 2R_b^2(1 - \cos\phi') + 2aR_b(1 - \cos\phi')\cos\theta'$, where θ' is a local variable around the circular cross-section of the loop element. Here the

$$\int_{-h}^{+h} I(z')G(z,z')dz' + C\cos(kz) = \frac{1}{j\eta}\int_0^z E_i(z')\sin(k(z - z'))dz' \quad (5)$$

$$\int_{c'}\int_{s'} J(s')\left[G(s,s') - k\int_0^s \sin k(s - \xi)G(\xi,s')(1 - \hat{\xi}\bullet\hat{s}')d\xi\right]ds' + C\cos ks = \frac{1}{j\eta}\int_0^s (\bar{E}_i\bullet\hat{\xi})\sin k(s - \xi)d\xi \quad (6)$$

where $G(z,z') = \frac{1}{4.\pi}\int_{\phi'=0}^{2\pi}\frac{e^{-jkR}}{R}d\phi'$

Extended Boundary Condition is used and the net electric field on the axis of the loop is zero. The numerical solutions for I in equations (5) and (6), which are expressed in the usual $ZI = V$ system, are obtained with the aid of the Boundary Residual Method, BRM, [15][16]. This is a Least Squares Method variant that has two important elements. The first significant element is that the entries in the Z and V matrices are calculated as they would be for a point-matching method. However the location of the matching points is not arbitrary. Specifically they are located at the nodes of an appropriate integration rule such as Gauss-Legendre. Furthermore, the number of sample points exceeds the number of free variables, typically by a ratio of 2:1 or higher. This means the Z matrix is rectangular and the matrix equations are solved using QR or SVD methods [17]. The second important element is that the rows in the Z and V matrices are weighted by the weights from the same integration rule used to establish the nodes mentioned earlier. This has the important result of minimizing the residuals integrated over the entire surface being studied. Formally, this statement is min $\rho_{LS}^2 = \|ZI - V\|_2^2$. This is an important measure. It reports on the performance of the solution over the complete surface and hence it is referred to here as a global measure. For comparative purposes, it is best to normalize this function. The normalized residual is:

$$\rho_{norm}^2 = \frac{\|ZI - V\|_2^2}{\|V\|_2^2} \tag{7}$$

The Dipole as a Scatterer.

In order to calculate the currents on a straight dipole excited by a plane wave equation (5) is evaluated in conjunction with the basis functions shown in Table I. The boundary condition, $I(\pm h) = 0$, is satisfied in one of three ways. In the first method a_1 and a_{N+1} are set to zero. In the second approach, the two end cells support the basic/conventional end function $I(z') = a_0\sqrt{(h - |z'|)/\Delta}$ and then enforce $a_0 = a_1 = a_{N+1}$. The derivatives, b_1 and b_{N+1} and higher, are left unconstrained. In the third approach, the special Hermite end splines defined earlier are used and all applicable constraints are enforced. In the case of the linear spline, the second and third approaches utilize the same function. For the quadratic case, a two term end spline is used, for the cubic case a three term end spline is used and the quartic spline employs a four term end spline. The plane wave is polarized parallel to the axis of the dipole and is normally incident.

Figure 1a shows the results for the current at the center of a half-wave dipole, with a radius of 0.007λ. As the order of the spline is increased the results without the inclusion of any special end sections show only a small benefit from the inclusion of higher order terms. The inclusion of the conventional end spline provides an improvement, particularly for the lower order splines. Interestingly, the convergence curves for all four splines look very similar. It is only when the Hermite type end splines are added that the real benefit of using high order splines is observed.

Figure 1b reports the results for the Normalized Residual. It is observed that the conventional end function improves the performance of the lower order basis functions. However, the performance of the Hermite end functions is consistently better.

The Loop Antenna.

As mentioned above, the circular loop is used to investigate the discontinuity associated with a magnetic frill. The basis functions defined in equations (4a) and (4b) are used in conjunction with equation (6) to evaluate the currents at the feed-point of the antenna. When using equation (4b) the value of N is only half that of the corresponding value used with equation (4a). The circumference of the loop is one wavelength and $\Omega = 2\ln(2\pi R_b / a) = 10.0$, where R_b is the radius of the loop and a is the radius of the loop element.

The convergence curves for the central current are shown in Figure 2a and the associated normalized residuals are shown in Figure 2b. The results show clearly the superiority of a series that accommodates the ‘charge jump’ at the feed-point, thereby confirming the presence of the phenomenon. Only 32 terms are considered in these graphs. If the number of terms were increased substantially, the results for the cosine series only would eventually converge to those observed with the use of the supplemented basis functions.

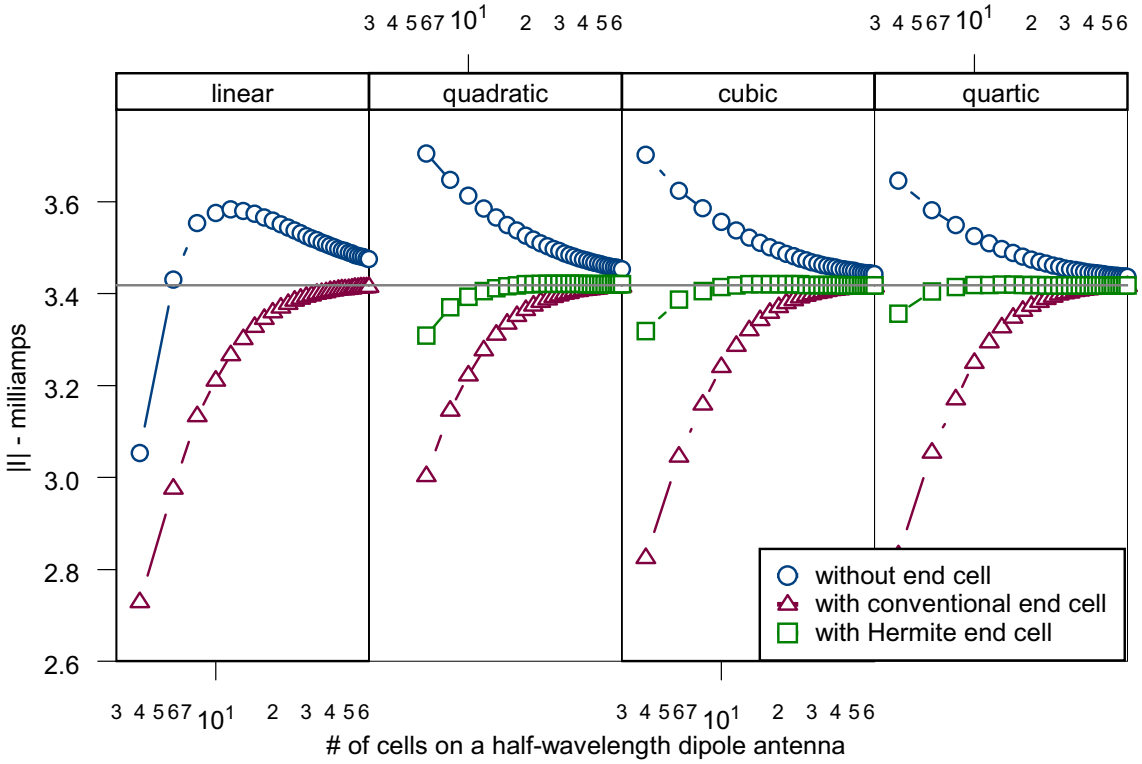

Figure 1a. Plots of the current on a dipole excited by a plane wave modeled with four splines

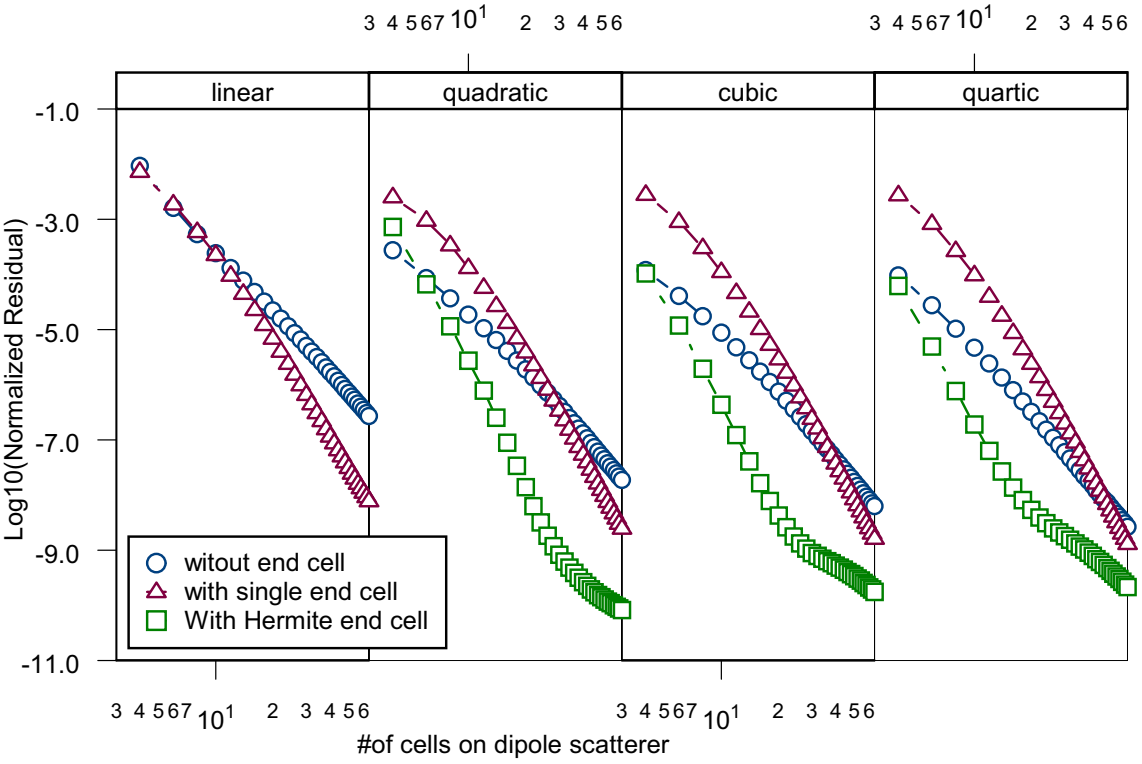

Figure 1b. Plots of the normalized residual on a half-wave dipole excited by a plane wave.

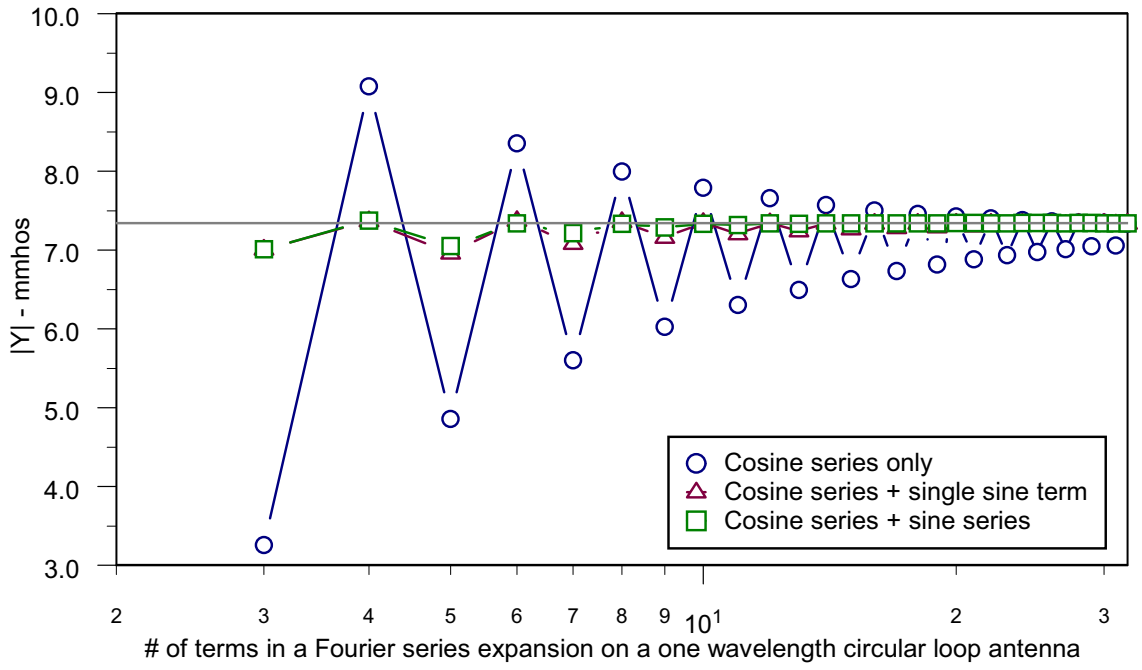

Figure 2a. Plots of the input admittance of a circular loop excited by a magnetic frill.

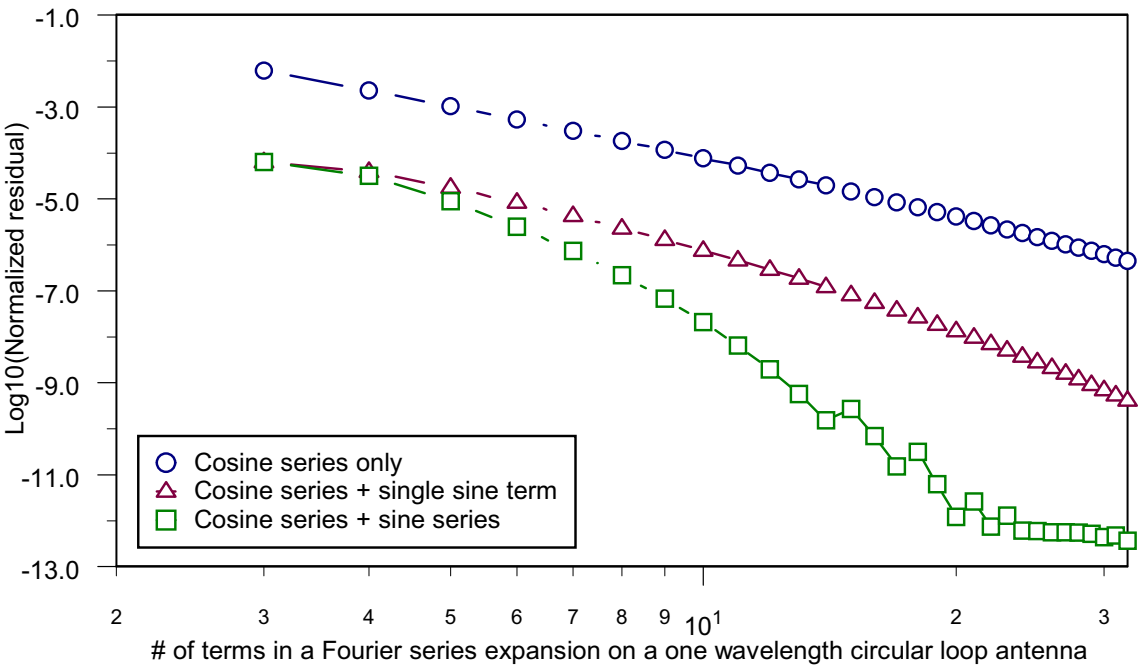

Figure 2b. Plots of the normalized residual for a circular loop excited by a magnetic frill.

$$I = a_0 + \sum_{i=1}^{N} a_i \cos(i\pi z'/h)\sqrt{h - |z'|} \quad (8a)$$

$$I = a_0 + \sum_{i=1}^{N} \left(a_i \cos(i\pi z'/2h) + b_i \sin((2i-1)\pi |z'|/2h) \right)\sqrt{h - |z'|} \quad (8b)$$

The Dipole as an Antenna.

The dipole antenna incorporates both of the types of discontinuity already discussed. Here, it has radius, a, of 0.007λ. The frill has dimension of b/a=2.3 where b is the outer radius of the frill. The combination of these two discontinuities is explored initially using sub-domain functions. The sub-domain functions are the same as those used earlier with a dipole scatterer. However, at the center of the dipole, the phase in the terms representing the first and third derivatives is shifted 180^0 when these derivatives exist. The impact on the convergence of the current at the feed-point can be seen in the results reported in Figure 3a. The results for the associated normalized residuals are shown in Figure 3b. It is clear, from both sets of data, that the phase reversal of the odd order derivatives at the frill contributes significantly to an improved model for the current.

Entire-domain functions have long been used to model the current on a linear dipole antenna. A study that compared ten such functions was published recently [18]. That study concluded that entire-domain functions performed poorly on the linear dipole. Historically, however, the choice for an entire-domain function on a linear dipole has been one of various forms of a Fourier series. In the absence of a better alternative, such a series is used here. The particular form of the Fourier series used is shown in (8a) above. In order to accommodate the "charge jump" at the magnetic frill, a modified form of the latter was investigated – this is shown in (8b) above.

The results, for the input admittance of a half-wavelength antenna, using these two series are shown in Figure 4a. The corresponding findings for the normalized residuals are shown in Figure 4b. When using equation (8b) the value of N is only half that of the corresponding value used with equation (8a). Both figures clearly demonstrate the utility of incorporating terms that address the issue of discontinuity across the frill.

Discussion.

End Effects. When considering the results reported in Figure 1a, one must bear in mind that, for the linear spline, the conventional end term and the Hermite end term are one and the same. Adding a single end term to any of the splines produces an observable improvement in the convergence of the current at the center of the dipole compared with not using one at all. This is particularly true for the lower order splines. As mentioned earlier, the convergence curves obtained when using a single conventional end term all appear to have the same convergence characteristics. This suggests that the end term is limiting the convergence process. When the higher order end terms are included, to the maximum order possible, the convergence process is speeded up significantly. When viewed from a global perspective, as reported in Figure 1b, the conventional end term is important in the case of the linear spline. For the higher order splines the benefits become less as the order of the spline is increased. However, when the higher order end terms are included, the global results are distinctly better for all splines.

Magnetic Frill. The importance of properly incorporating "charge jump" properties into models of current flowing on an antenna excited by a magnetic frill is dramatically illustrated in Figures 2-4. The significant oscillations seen when employing a Fourier series containing only cosine terms is an indication of its lack of suitability – for both the loop and the linear dipole! To be sure that the oscillations were the result of the feed mechanism and nothing else, the excitation was changed from the magnetic frill to a plane wave. The oscillations disappeared in the case of the loop and were highly attenuated on the linear dipole. This allowed the conclusion that the oscillations are indeed a result of using the magnetic frill excitation and not something else. The addition of the sine terms in the current model, while improving the convergence results significantly, does raise the condition number of the impedance matrix from the region of $\sim 10^4$ up to

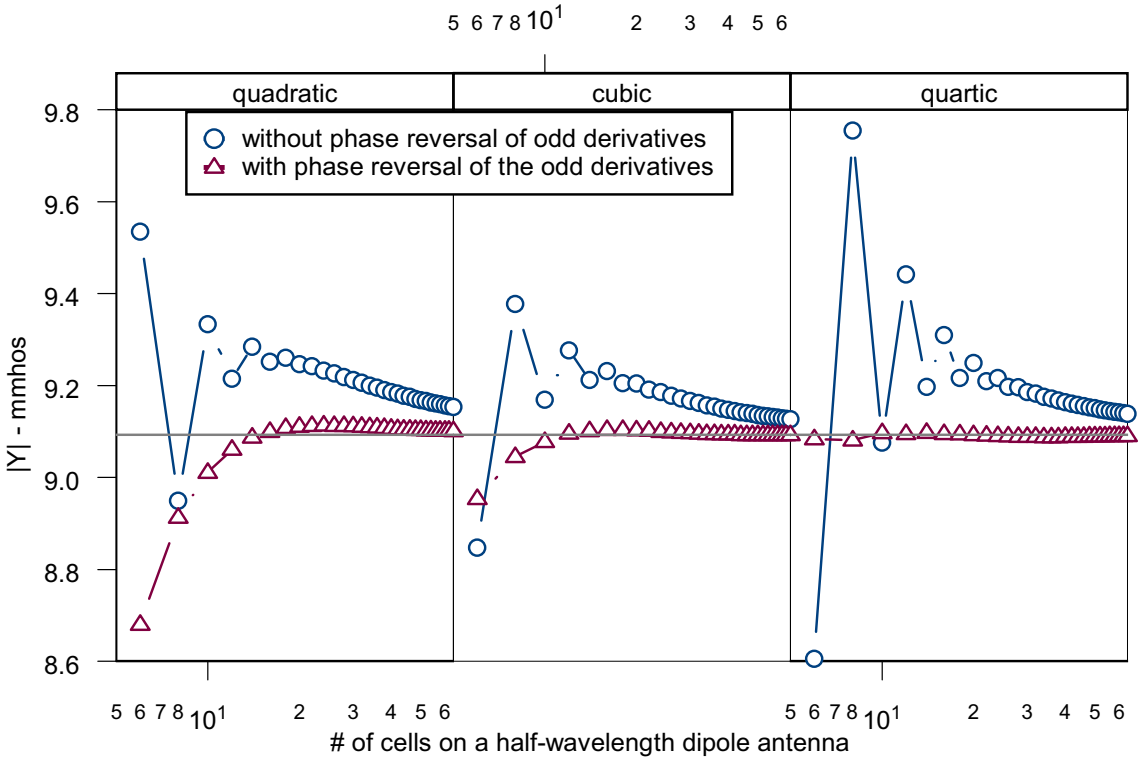

Figure 3a. Plots of admittance on a dipole excited by a magnetic frill for three splines.

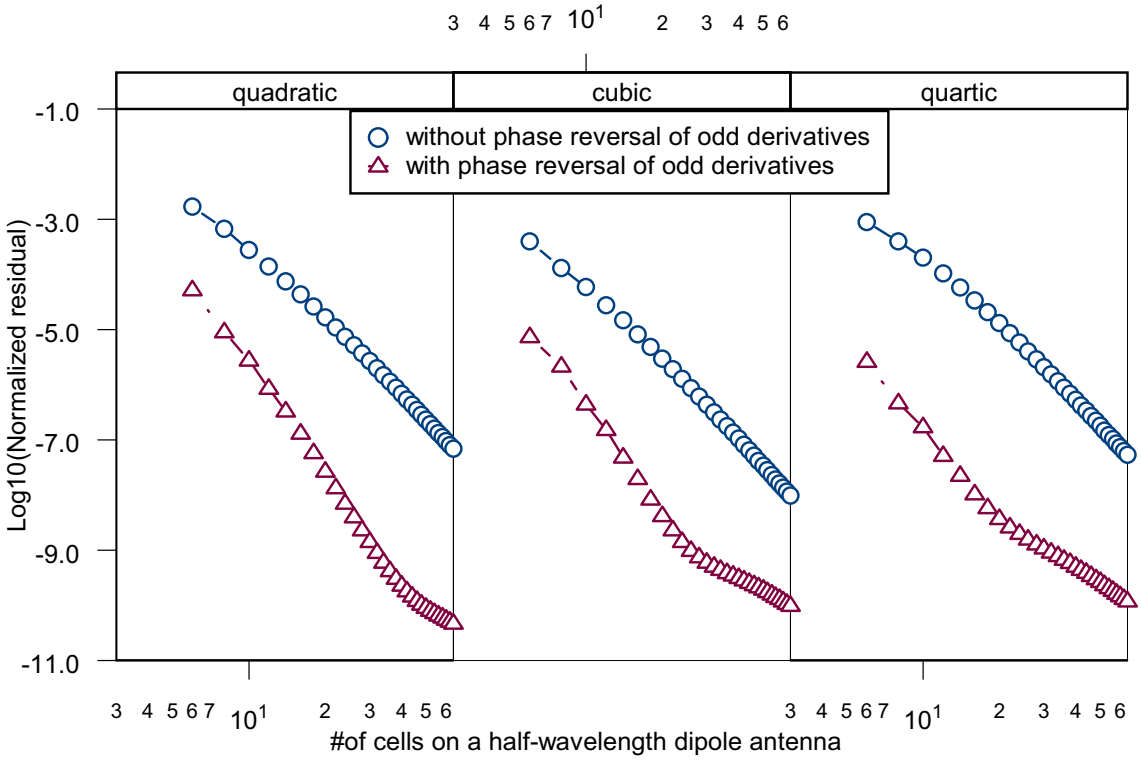

Figure 3b. Plots of the normalized residual on a dipole with magnetic frill for three different splines.

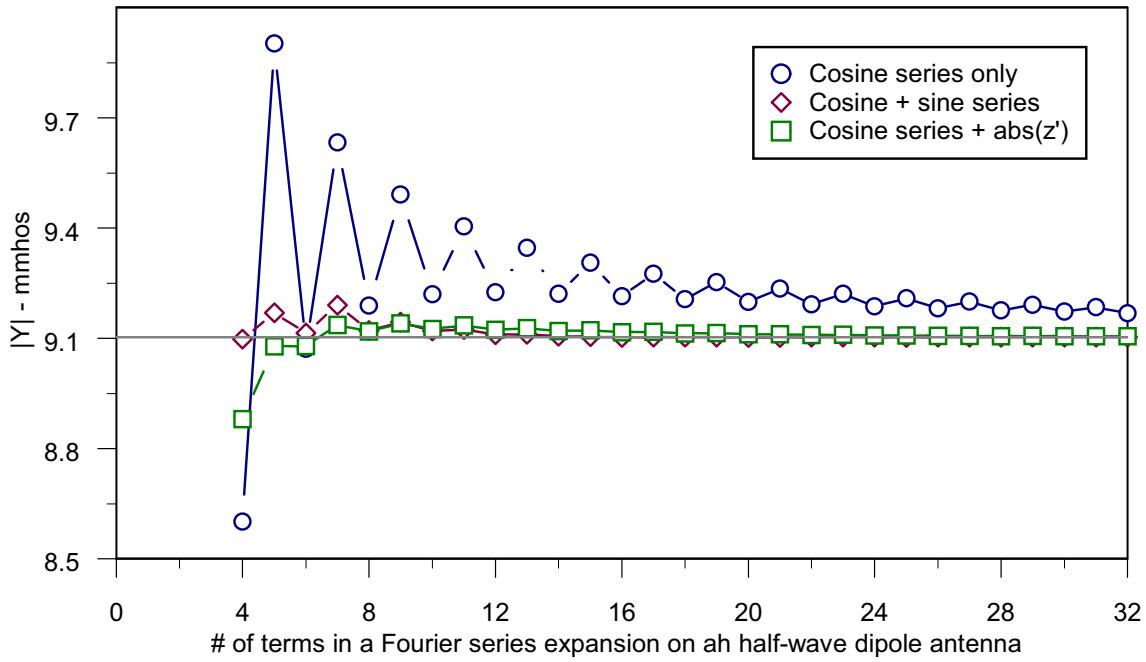

Figure 4a. Plots of the admittance of a half-wave dipole excited by a magnetic frill

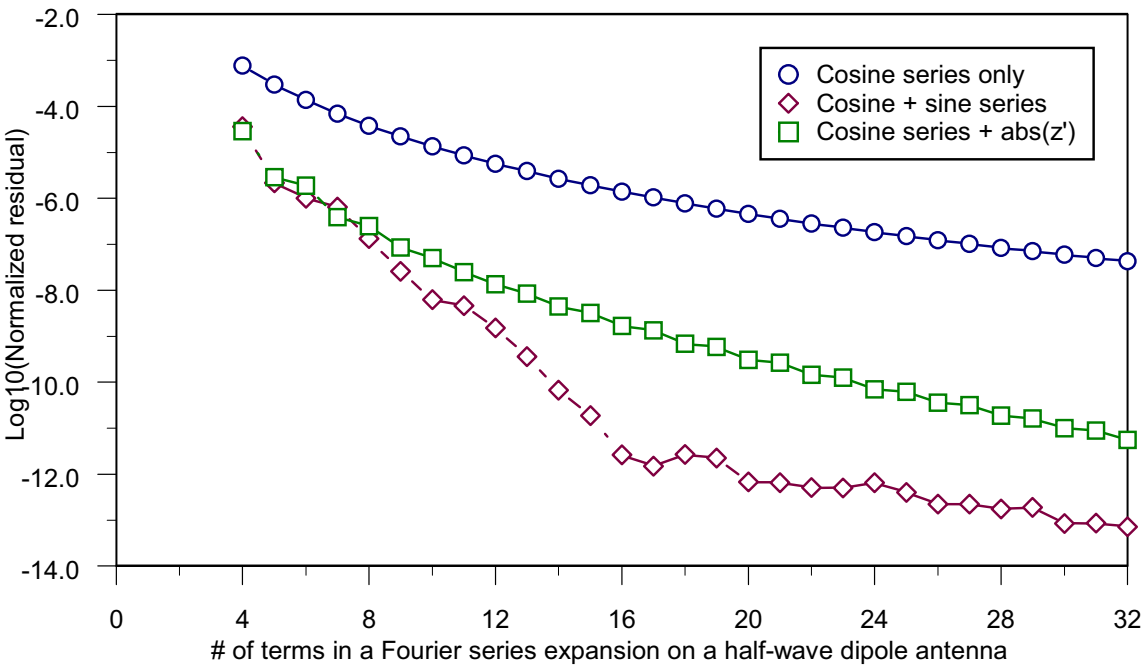

Figure 4b. Plots of the normalized residual on a half-wave dipole excited by a magnetic frill

$\sim 10^{10}$ when more than 12 terms are used in the series.

The linear dipole problem was also solved using a Method-of-Moments solution, using the standard Pocklington equation. This was done as a check on the testing method and the integral equation formulation. The testing functions were pulses of equal dimensions, the basis functions were again the Fourier series of (8a) and (8b) and the Pocklington equation was regularized per the procedure described in [19]. The results of using (8b) converged significantly faster than when using (8a) while the oscillations noted in connection with Figure 4 were almost completely attenuated. These findings provided further confirmation of the need to accommodate the discontinuity at the feed-point.

The presence of a high condition number in the entire domain solutions that include a series expansion of the absolute value of sine terms makes them unattractive. Consequently, the effect of incorporating a single term only was investigated. In the case of the loop this term was $\sin(|\phi'|/2)$. In the case of the dipole it was simply $|z'|$. The associated results are shown in Figures 2 and 4 respectively. Use of just these single terms contributes significantly to alleviating the convergence problem. The condition numbers were comparable to those observed when using the cosine terms only. This suggests that one judiciously selected term could significantly speed up the convergence rate in these situations. However, the ones tested here are not those functions – otherwise they would exhibit normalized residual curves at least as steep as those shown by the addition of the sine series.

The basic EFIE for a loop is shown in equation (9a). After some manipulation, this assumes the form shown in (9b). When the current is represented by (4a) the form in (9c) results. The last term on the right-hand side of this latter equation evaluates to zero. But this is the term that represents the "charge jump". Therefore the representation of (4a) is inadequate. A term, or terms, that permit(s) the current derivative at the origin to be discontinuous is necessary. The inadequacy of the representations of (4a) and (8a), is believed to be the main source of the oscillations seen in the relevant convergence curves.

In 1980, Richmond [20] reported that the incorporation of a term that represented an outgoing wave on an infinite dipole improved convergence considerably on a finite dipole. This was confirmed in [18], where it was also noted that the condition numbers were high. This outgoing term is essentially a log term at the feed-point and consequently presents a discontinuity there. It is possible that this discontinuity had more to do with the improvement realized by Richmond than the form of the term itself.

Conclusions.

This study was motivated by the apparent failure of high-order basis functions to improve convergence rates when compared with basis functions of lower order [6][7]. As a result of this work, it is believed that the reasons for this failure originate with inadequate current modeling in the vicinity of discontinuities. Specifically, it has been demonstrated that to achieve superior convergence properties one must bear in mind three things.

1. Current models in the vicinity of discontinuities must support the same level of continuity as that supported by the models employed away from the discontinuities.
2. When an isolated excitation source, such as a magnetic frill, is part of the system, the current model(s) must have sufficient flexibility to accommodate issues such as "charge jump" in the excitation region.
3. The above comments apply to both sub-domain and entire-domain models.

$$\frac{E_i(\phi)}{j\omega\mu} = \int_{-\pi}^{\pi} \cos(\phi - \phi')I(\phi')G(\phi,\phi')Rd\phi' + \frac{1}{k^2R^2}\int_{-\pi}^{\pi}\frac{dI}{d\phi'}\frac{dG}{d\phi}Rd\phi' \quad (9a)$$

$$\frac{k^2R}{j\omega\mu}E_i(\phi) = \left[\left(\int_{-\pi}^{0-} + \int_{0+}^{\pi}\right)\right]\left(\cos(\phi - \phi')k^2R^2I(\phi') + \frac{d^2I}{d\phi'^2}\right)Gd\phi' + \frac{dI}{d\phi'}G\Big|_{0-}^{0+} \quad (9b)$$

$$\frac{kR}{j\eta}E_i(\phi) = \left[\left(\int_{-\pi}^{0-} + \int_{0+}^{\pi}\right)\right]\left(\cos(\phi')k^2R^2a_0 + \sum_{j=1}^{N}(\cos(\phi')k^2R^2 - j^2)a_j\cos(j\phi')\right)Gd\phi' + \sum_{j=1}^{N} -ja_j\sin(j\phi')G\Big|_{0-}^{0+} \quad (9c)$$

Acknowledgements.

The author thanks Professor Andrew Peterson of the Georgia Institute of Technology for his encouragement and useful suggestions in connection with the preparation of this paper.

References.

[1] L. Meixner, "The Behavior of Electromagnetic Fields at Edges", *IEEE Trans. on Ant. & Prop.,* Vol. 20, No. 4, pp.442-446, 1972.

[2] J. Van Bladel, *Singular Electromagnetic Fields and Sources*, Chapter 4, Clarendon Press, 1991.

[3] H. Shen and T. T. Wu, "The Universal Current Distribution Near the End of a Tubular Antenna", J. Math. Phys., 30(11), Nov., 1989.

[4] H. Shen, R. W. P. King and T. T. Wu, "The Combination of the Universal End-Current and the Three-Term Current on a Tubular Dipole", J. of Electromagnetic Waves and Applications, Vol. 4, No. 5, 189-200, 1990.

[5] B. D. Popovic, M. B. Dragovic and A. R. Djordjevic, *Analysis and Synthesis of Wire Antennas*, Research Studies Press, 1982.

[6] M. M. Bibby, "A Comparative Study of Expansion Functions Using the Boundary Residual Method on a Linear Dipole – Part II: Sub-Domain Functions", *Journal of the Applied Computational Electromagnetic Society*, Vol. 17, No. 1, pp. 54-62, March 2002.

[7] M. M. Bibby, "An adaptive Approach to Faster Convergence in the Solution of Electromagnetic Problems by Using non-Uniform Cell Sizes", *Proc. 18th. Annual Review of Progress in Applied Computational Electromagnetics*, pp. 457-463, Monterey, CA., March, 2002.

[8] C. F. Gerald, *Applied Numerical Analysis*, 2nd. Ed., pp. 477-482, Addison-Wesley Publishing Co., 1978.

[9] J. F. Epperson, *An Introduction to Numerical Methods and Analysis*, pp. 171-181, John Wiley & Sons, 2002.

[10] M. M. Bibby, "Hermite Splines and Their Application in Electromagnetic Problems", in preparation.

[11] R. W. P. King, & G. S. Smith, *Antennas in Matter*, pp. 529-537, The MIT Press, 1981.

[12] G. Zhou & G. S. Smith, "An Accurate Theoretical Model for the Thin-Wire Circular Half-Loop Antenna", *IEEE Trans. on Ant. & Prop*., Vol. 39, No. 8, pp1167-1177, 1991.

[13] E. Hallen, "Theoretical Investigations into the Transmitting and Receiving Qualities of Antennae", *Nova Acta Regiae Soc. Sci. Upsaliensis*, Ser. IV, No. 4, pp. 1-44, 1938.

[14] K. K. Mei, "On the Integral Equations of Thin Wire Antennas", *IEEE Trans. on Ant. & Prop*., Vol. 13, pp. 374-378, May 1965.

[15] K. J. Bunch & R. W. Grow,, Numeric Aspects of the Boundary Residual Method", *Int. J. of Numerical Modeling: Electronic Networks*, Vol. 3, pp.57-71, 1990.

[16] K. J. Bunch & R. W. Grow, "On the Convergence of the Method of Moments, the Boundary Residual Method and Point-Matching Method with a Rigorously Convergent Formulation of the Point-Matching Method", *Journal of the Applied Computational Electromagnetic Society*, Vol. 8, No. 2, pp. 188-202, 1993.

[17] C. L. Lawson & R. J. Lawson, *Solving Least-Squares Problems*, Prentice-Hall, Inc., 1974.

[18] M. M. Bibby, "A Comparative Study of Expansion Functions Using the Boundary Residual Method on a Linear Dipole – Part I: Entire-Domain Functions", *Journal of the Applied Computational Electromagnetic Society*, Vol. 17, No. 1, pp. 42-53, March 2002.

[19] D. B. Miron, "The Singular Integral Problem in Surfaces", *IEEE Trans. on Ant. & Prop*., Vol. Ap-32, No. 3, May 1983.

[20] J. H .Richmond, "On the Edge Mode in the Theory of Thick Cylindrical Monopole Antennas", *IEEE Trans. on Ant. & Prop*., Vol. 28, No 6, pp. 916-920, Nov. 1980.

Malcolm M. Bibby received the B.Eng. and Ph.D. degrees in Electrical Engineering from the University of Liverpool, England in 1962 and 1965 respectively. He has been interested in the numerical aspects associated with antenna design for the last twenty years.